

Reversible magnetization and superconducting-state thermodynamic parameters for underdoped $\text{La}_{1.90}\text{Sr}_{0.10}\text{CuO}_4$

Yung M. Huh, J. E. Ostenson, F. Borsa, V. G. Kogan, and D. K. Finnemore

Ames Laboratory, U.S. Department of Energy and Department of Physics and Astronomy, Iowa State University, Ames, Iowa 50011

A. Vietkin and A. Revcolevschi

Laboratoire de Physico-Chimie des Solides, Universite Paris-Sud, Orsay, France

M.-H. Julien

Laboratoire de Spectrometrie Physique, Universite J. Fourier, BP 87, 38402 Saint Martin d'Herès, France

(Received 9 June 2000; published 22 January 2001)

Magnetization studies have been made of single-crystal $\text{La}_{1.90}\text{Sr}_{0.10}\text{CuO}_4$ with $H\parallel c$ in order to determine the magnitude of the flux expulsion and free energy in a material that has substantially less than optimal doping. Well above the superconducting transition temperature, the normal-state magnetization exhibits a two-dimensional Heisenberg antiferromagnetic behavior. Below T_c , there is a large portion of the H - T plane where the sample shows reversible behavior so that thermodynamic variables such as the free energy and the shape of the magnetization curves can be determined. At low temperature, the vortices have a well defined Abrikosov regime that transforms to two-dimensional fluctuation behavior at higher temperatures. The magnetization vs temperature curves show a unique crossing point at 22 K where the magnetization is independent of magnetic field. From this value of the crossing point, the effective layer spacing s is derived to be 1.6 nm compared to the CuO_2 lattice spacing of 0.66 nm. The fluctuations are found to obey two-dimensional scaling in that $M/(TH)^{1/2}$ is a universal function of $[T-T_c(H)]/(TH)^{1/2}$. Below 12 K, the data fit the Hao-Clem theory rather well and give κ_c values of about 175 and thermodynamic critical fields ranging from 112 mT at 12 K to 133 mT at 6 K.

DOI: 10.1103/PhysRevB.63.064512

PACS number(s): 74.40.+k, 74.60.-w, 74.70.-b

I. INTRODUCTION

Many of the high-temperature superconductors now can be prepared in single-crystal form with sufficiently high purity that there is a wide range of thermodynamic reversibility in the magnetization curves. From these measurements of reversible magnetization, the change in free energy with magnetic field can be determined from $G_n - G_s(H) = \int_0^H M_{sc} dH$. There is a very direct connection between reversible magnetization and free energy changes.

The underdoped high-temperature superconductor $\text{La}_{1.90}\text{Sr}_{0.10}\text{CuO}_4$ is a rather special material for the study of reversible magnetization and fluctuation diamagnetism because it still retains a relatively high transition temperature, and yet it also shows a substantial range of pseudogap behavior well above T_c .¹ As the sample is cooled, the pseudogap begins to open at about 600 °C and the material goes superconducting at $T_c \sim 30$ K. Optimum doping for this material occurs for a Sr content of about 0.15, so the single crystal under study here has about 2/3 the optimum number of charge carriers. There is a rich phase diagram in the H - T plane^{2,3} with several different changes in the vortex lattice. With the onset of superconductivity on cooling, quantized vortices first form in a liquid state, and then, with further cooling, this transforms to a variety of glasslike structures or regular lattice structures often depending on impurities and precipitates in the material. Important variables are the superfluid density, the anisotropy of the effective mass, $\gamma^2 = m_c/m_{ab}$, the entropy associated with the

flux-line lattice, and the nature of defects in the material. Changes in the flux-line lattice such as the melting transition are usually measured with transport properties,² but some of these changes may also be reflected in the free energy and in the shape of the reversible magnetization curves.

Some time ago, Kes and co-workers⁴ showed that the reversible magnetization curves, M vs H , of $\text{Bi}_2\text{Sr}_2\text{CaCu}_2\text{O}_{8+\delta}$, Bi-2212, have two rather different types of behavior depending on T . At low temperature, a plot of M vs H followed the classical Abrikosov⁵ rigid-lattice behavior with $|M|$ falling monotonically toward zero for fields larger than the lower critical field H_{c1} and smaller than the upper critical field H_{c2} . As the temperature rises, however, there are entropy terms^{4,6} in the free energy related to fluctuations in the flux-line lattice, and the reversible magnetization curves have been shown to have a crossover from Abrikosov-like⁵ behavior at low temperature to fluctuationlike behavior^{4,6} as the temperature approaches the transition temperature T_c . There is, in fact, a unique crossing point on the M vs T plot where M is independent of H . For Bi-2212, where the anisotropy ratio, $\gamma = [m_c/m_{ab}]^{1/2}$, is about 200, this crossover occurs at a reduced temperature of about $T/T_c = 0.95$.⁴ The data show magnetization vs temperature (M vs T) curves for various magnetic fields that cross at a single temperature, $T^* = 88.3$ K where M is independent of H . If these same data can be cast as M vs H curves, the curves show Abrikosov-like behavior well below 86 K, and fluctuationlike behavior above 86 K. In the fluctuation regime, Li *et al.*⁷ have shown two-dimensional (2D) scaling behavior for

$\text{Bi}_2\text{Sr}_2\text{Ca}_2\text{Cu}_3\text{O}_{10+\delta}$, Bi-2223 in that a plot of $M/(TH)^{1/2}$ is a universal function of $(T-T_c)/(TH)^{1/2}$. In addition, Welp and co-workers⁸ have shown three-dimensional, 3D, scaling behavior for $\text{YBa}_2\text{Cu}_3\text{O}_{7-\delta}$, Y-123, in that $M/(TH)^{2/3}$ is a universal function of $[T-T_c(H)]/(TH)^{2/3}$. Theoretical work by Tesanovic and Andreev⁹ have worked out these closed form relations for the scaling in both 2D and 3D.

Oxygen depletion is a standard way to alter the superfluid density and thus possibly increasing the 2D behavior in these high-temperature superconductors. This is illustrated by the work of Janossy *et al.*¹⁰ who have shown that the effective-mass ratio, $\gamma=[m_c/m_{ab}]^{1/2}$, can be raised in $\text{YBa}_2\text{Cu}_3\text{O}_{7-\delta}$ from about 5 to 25 by depleting the oxygen content from ~ 7.0 to ~ 6.5 . Depleting oxygen, or underdoping, then may be a method to transform a superconductor from 3D to 2D behavior. In addition to the work with Y-123, this group also has shown that optimally doped $\text{La}_{1.85}\text{Sr}_{0.15}\text{CuO}_4$ has an anisotropy ratio of about $\gamma\sim 10$ to $\gamma\sim 20$, and Willemin *et al.* have shown that $\text{La}_{1.90}\text{Sr}_{0.10}\text{CuO}_4$, has $\gamma=43$.¹¹ Hence $\text{La}_{1.90}\text{Sr}_{0.10}\text{CuO}_4$, might be expected to show a cross-over from Abrikosov-like magnetization curves to fluctuationlike magnetization curves at a relatively low reduced temperature.

Two other cases where the magnetization curves resemble the fluctuationlike behavior are the stripe phase superconductor, $\text{La}_{1.45}\text{Nd}_{0.40}\text{Sr}_{0.15}\text{CuO}_4$,^{12,13} and Bi-2212 with a dense array of columnar defects.¹⁴ For the $\text{La}_{1.45}\text{Nd}_{0.40}\text{Sr}_{0.15}\text{CuO}_4$ sample, M vs H curves show fluctuationlike curves at reduced temperatures as low as $T/T_c=0.5$. For the Bi-2212 sample with columnar defects,¹⁴ the crossover point disappears. In addition, many of the vortex cores reside on the columnar defects thus altering the field dependence of the magnetization.

The purpose of this work is to study the shape of the magnetization, M vs H , curves for underdoped La-214 in order to determine the free energy of the vortex lattice and the temperature range over which fluctuation behavior is observed. To do this, it is necessary to determine the normal-state magnetization¹⁵ above T_c to confirm that the Cu spins follow a 2D Heisenberg antiferromagnetic behavior¹⁶ and to obtain analytical fits to subtract background. Several different spin configurations and models can give a susceptibility that slowly decreases as the temperature decreases¹⁷ as is seen here. If one assumes that the superconducting transition does not change the configuration of the background spin susceptibility, then the superconducting flux expulsion can be obtained from the measured total magnetization by subtracting the normal-state background. This procedure, of course, only makes sense if the magnetization is thermodynamically reversible, so it also is important to establish the irreversibility line, H_{irr} vs T and verify that there is a large reversible region in the H vs T plane. Reversible magnetization data are then fit to a theoretical model to estimate the thermodynamic critical field curve. A secondary goal of the work is to look for diamagnetic fluctuations at temperatures well above T_c in the regime normally called the pseudogap regime. This is difficult because the signal becomes progressively smaller as T increases and the signal gradually disappears into the background magnetization.

II. EXPERIMENT

The single crystal used in these measurements was prepared by a floating zone method in an image furnace,¹⁸ and it is the same crystal used for NMR spin-lattice relaxation studies.¹⁹ X-ray photographs were taken at several places on the surface of the crystal to establish that it was a single crystal and the c axis was found to be perpendicular to one of the cleavage planes. Magnetization data were taken with $H\parallel c$ in a Quantum Design superconducting quantum interference device magnetometer over the full range of temperatures from 4.5 to 200 K and magnetic fields up to 7 T.

III. RESULTS AND DISCUSSION

From 55 to 200 K, where the sample is normal, the magnetization is of the form

$$M = CH + M_s \tanh(\beta H), \quad (1)$$

as shown in Fig. 1. The inset shows the behavior at low field and the solid lines are the fits to Eq. (1).

Results show that $4\pi M_s = 0.060 \pm 0.001$ G and $\beta = (8.15 \pm 1.54) \times 10^{-4}$ G⁻¹ over the whole temperature range so the second term in Eq. (1) is independent of temperature. Over most of the H - T plane, this whole term is small compared to both CH and the superconducting magnetization. This means that there is a small ‘‘ferromagnetic’’ moment parallel to the c axis that saturates at a few tenths of a Tesla and remains constant over the entire temperature range.

Values of C , which is the dimensionless volume susceptibility, range from 1.32×10^{-6} at 200 K to 8.76×10^{-7} at 55 K and are close to those measured by Nakano *et al.*²⁰ and Johnston¹⁵ in this range of doping. Hence the normal-state magnetization follows 2D Heisenberg antiferromagnet behavior rather well.

To subtract the background magnetization at lower temperatures, we follow the lead of de Jongh¹⁷ and assume that magnetization from the Cu spins continues to follow 2D antiferromagnetic behavior at temperatures below 40 K. Values of $C(T)$ are obtained by linearly extrapolating the C vs T curve between 200 and 55 K to lower temperature. To investigate worst cases for background subtraction, two other assumptions about the temperature dependence of C have been made: (i) C falls linearly to zero as T goes to zero, (ii) C rises about 20% above the 40-K value as T goes to zero as happens for some antiferromagnets.¹⁶ The normal-state background is small enough that the basic conclusions about the thermodynamic critical field line are not changed within ± 1 mT.

With the assumption that the onset of superconductivity does not alter the magnetization of the Cu spins, and the superconducting magnetization M_{sc} is derived from $M_{sc} = M_t - M_b$, where M_t is the total magnetization and M_b is the background magnetization. At 16 K and 5 T, the background is about 20% of the total magnetization. A study of the irreversibility shows that H_{irr} rises from zero at 28 K to

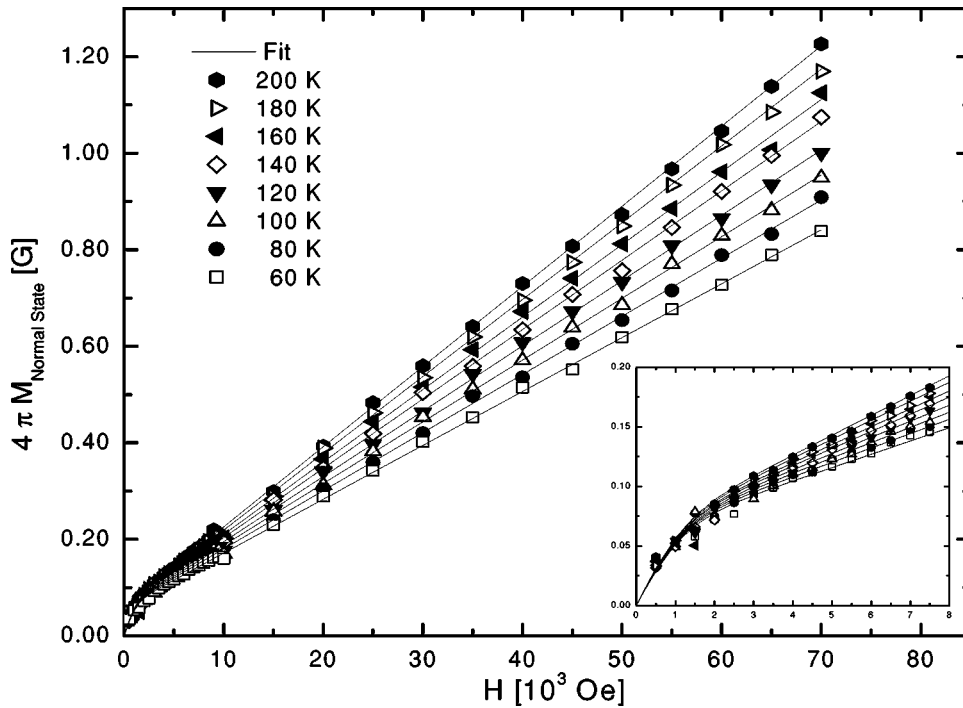


FIG. 1. Normal state magnetization every 20 K from 60 to 200 K. The solid lines are fits of the data to Eq. (1). The inset expands the low-field portion.

0.5 T at 15 K, 1.0 T at 10 K, and 2.5 T at 6 K. Hence there is a wide range of thermodynamic reversibility in the H - T plane.

Superconducting magnetization curves are shown for every 2 K from 8 to 30 K in Fig. 2. All of these data are in the region of thermodynamic reversibility. Below 18 K, the M vs H curves monotonically approach zero from the negative side in a fashion similar to an Abrikosov type-II superconductor.⁵ Above 22 K, the magnetization rises from zero at $H=0$ similar to fluctuation behavior.⁴ If these same data are cast as M vs T , as shown in Fig. 3, there is a crossing point just above 22 K where the curves cross and the magnetization is independent of H .^{4,6} At the crossover temperature T^* the magnetization is given by $-M^* = k_B T^* / \phi_0 s$.⁶ Using $T^* = 22.0$ K and $4\pi M^* = -1.13$ G gives an effective

layer spacing, $s = 1.6$ nm compared with the CuO_2 plane spacing of 0.66 nm. It is possible that the $s = 1.6$ -nm value from these measurements arises because only part of the sample is superconducting thus giving rise to smaller M^* values as described by Kogan *et al.*²¹ With this interpretation, the ratio of 0.66 nm/1.6 nm gives 41% of this underdoped $\text{La}_{1.90}\text{Sr}_{0.10}\text{CuO}_4$ sample being superconducting. In a closely related measurement, Iwasaki *et al.* found a value of $s = 1.49$ nm for $\text{La}_{1.92}\text{Sr}_{0.08}\text{CuO}_4$.²² In addition, Mosqueira *et al.*²³ have studied the crossover in $\text{La}_{1.90}\text{Sr}_{0.10}\text{CuO}_4$ for grain-aligned powders. They find $T_c = 28$ K, $aT^* = 25$ K, and essentially the same M^* as seen here.

The crossover feature that is well obeyed from 0.5 to 7 T is not obeyed in the low flux density limit of 0.001 T or 1 mT. As shown by the solid line in Fig. 3, an M vs T curve

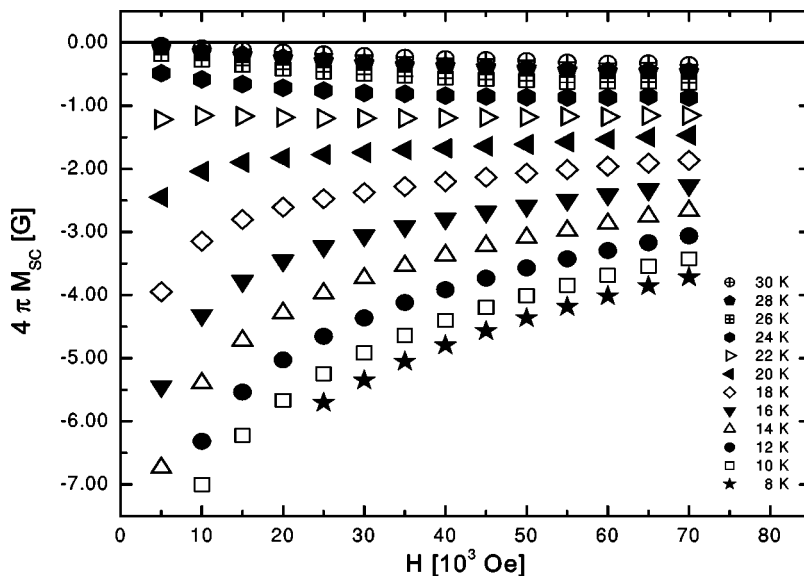


FIG. 2. Superconducting magnetization curves every 2 K from 8 to 30 K showing Abrikosov-like behavior below 18 K and fluctuationlike behavior above 22 K.

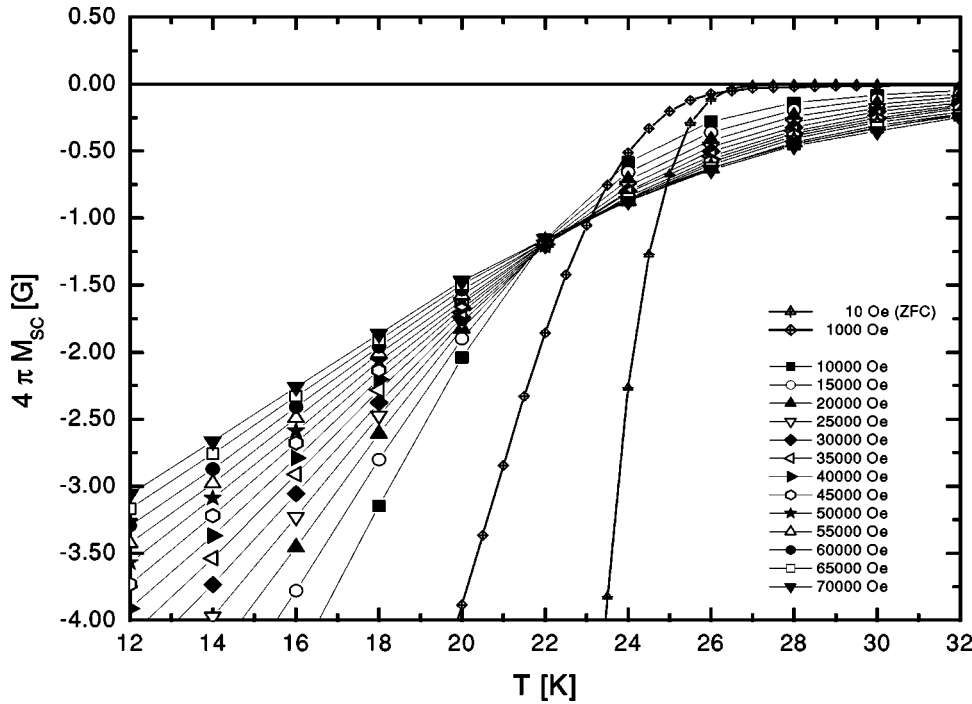


FIG. 3. Magnetization vs temperature showing the crossover at 22 K. Data are plotted every half Tesla from 1.0 to 7.0 T.

taken at 1 mT deviates from zero somewhere in the 26–27-K range. The curve shown for 0.1 T also misses the crossing point. A 1-mT magnetization run is often used to define a T_{co} , the mean-field transition temperature, and for this sample, a temperature more like 26.5 K. This would imply that for this sample, T_{co} is about 5 K above T^* .

There is a substantial amount of fluctuation diamagnetism all the way up to 30 K, as shown in Fig. 3, that might be fit to fluctuation theories.⁸ Even at 30 K, the magnetization is still increasing with increasing field all the way up to 7.0 T, as shown in Fig. 2. If the data are plotted as $M/(TH)^{1/2}$ vs $[T - T_c(H)]/(TH)^{1/2}$, the data lie on a common curve as

shown in Fig. 4. In this analysis, $T_c(H)$ is determined by taking $T_{co} = 26.8$ K from the Hao-Clem fits to these data and by taking the slope of $dH_{c2}/dT = -3.20$ T/K from Eq. (13) of Tesanovic *et al.*⁹ Attempts to fit to 3D scaling gave less good fits.

In an attempt to make a reasonable estimate of the thermodynamic critical field, each of the magnetization curves in Fig. 2 were fit to theoretical models for the magnetization in three different ways. The Hao-Clem model²⁴ is a variational calculation that includes the energy of the core of the vortices and uses H_c and κ_c as adjustable variables. All of the data reported in these measurements are far from H_{c2} so the

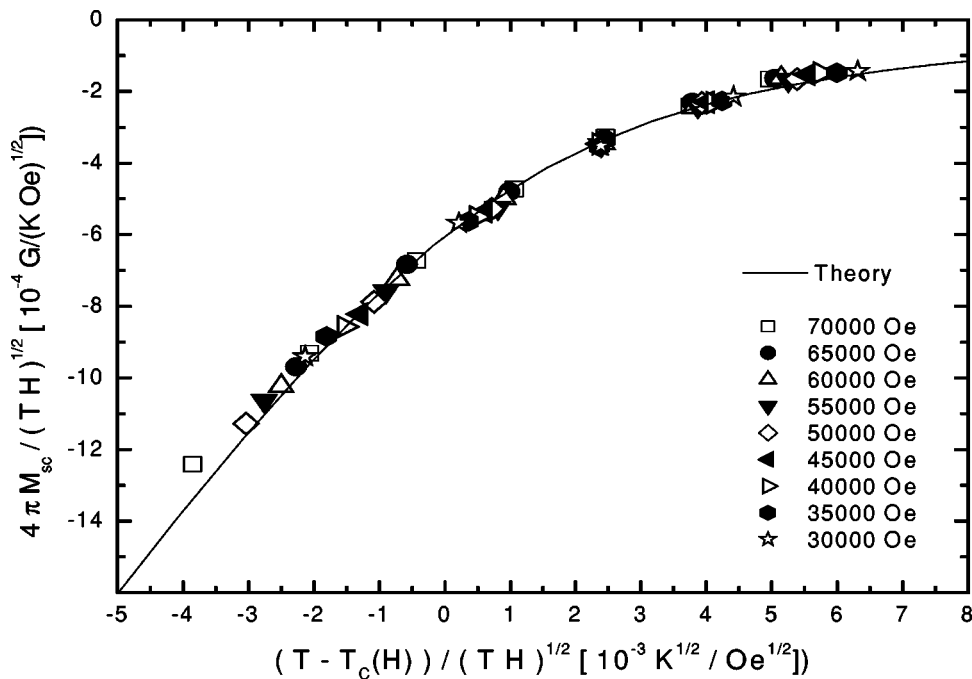


FIG. 4. 2D scaling behavior of the magnetization every half Tesla from 3.0 to 7.0 T.

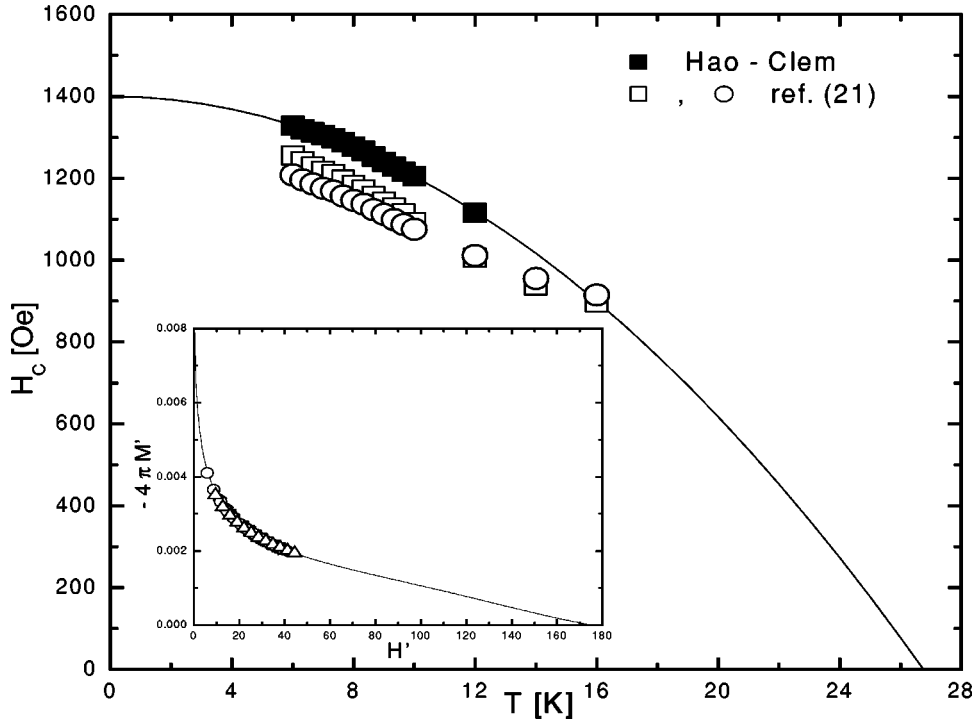


FIG. 5. Thermodynamic critical field H_c vs T determined three different ways. The inset shows a fit of the data from 6 to 12 K to the universal Hao-Clem curve for $\kappa_c=175$.

fit gives an uncertainty of about 10% in κ_c . Selecting the average value of $\kappa_c=175$ for all temperatures, the data have been fit to the universal Hao-Clem curve with just H_c as the adjustable parameter with the results shown in Fig. 5. If both κ_c and H_c are taken as variables, the fits can be improved slightly, but the data are not close enough to H_{c2} to realistically evaluate κ_c better than this average value. As shown in the inset of Fig. 5 where the dimensionless variables $M' = M_{sc}/\sqrt{2}H_c$ and $H' = H/\sqrt{2}H_c$ are plotted, the data fit the Hao-Clem²⁴ model rather well with the H_c values ranging from $H_c=133$ mT at 6 K to $H_c=112$ mT at 12 K. These H_c values are plotted as solid squares in Fig. 5. If these are fit to a parabolic critical field curve, $H_c=H_o[1-(T/T_c)^2]$, one finds $H_o=0.140$ T and $T_{co}=26.8$ K. The slope dH_{c2}/dT from these fits gives -2.6 T/K at T_c in reasonable agreement with the value derived from Tesanovic⁹ of -3.2 T/K. These data also are to be compared with a previous study by Li *et al.*²⁵ who found $H_o=0.143$ mT and $T_c=28.23$ K for an $x=0.092$. They also found $H_o=0.251$ mT and $T_c=34.39$ K for an $x=0.154$ sample at essentially optimum doping. If a straight line is drawn on an H_o vs x plot from the optimum-doped sample through the datum for this sample, H_o would extrapolate to zero at $x \sim 0.03$. The current H_c vs T results then are in good agreement with these previous data.²⁵

An alternate way to determine H_c is to use the theory of Kogan *et al.*²¹ that is based on London theory and takes more full account of the entropy associated with the fluctuations. In the first method, we determine s from the crossing measurements by, $s = -k_B T^*/\phi_o M^* = 1.66$ nm, assuming that $\ln[\eta\alpha\sqrt{e}] = 1$. Then we fit the M vs H data to Eq. (1) in Kogan *et al.*²¹ to give the best values of κ_c and λ_{ab} . From these, we calculate the H_c values shown by the open squares of Fig. 5.

In the second method that uses the Kogan *et al.* approach, we assume that $s=0.66$ nm given by the copper-oxide plane spacing and determine $\ln[\eta\alpha\sqrt{e}]$ from $-M^* = [k_B T^*/\phi_o s]\ln[\eta\alpha\sqrt{e}]$. Inserting these values into Eq. (1) of Kogan *et al.* and fitting the data gives $H_{c2}(T)$ that can be converted to the H_c values shown by the open circles of Fig. 5.

The central result of these various methods to determining H_c from the M vs H data is that all the methods give roughly the same result. An extrapolation of the Hao-Clem H_c vs T data (solid squares of Fig. 5) gives $T_{co}=26.8$ K in reasonable agreement with the temperature where the 1.0 mT M vs T curve breaks away from zero. Extrapolating the second Kogan method (open circles of Fig. 5) gives about 27.4 K. All of the H_c data of Fig. 5 indicate a ratio of $H_c(0)/T_{co} = 5.4$ mT/K.

Magnetization curves were measured as a function of the polar angle away from $H\parallel c$ to determine how sensitive the magnetization was to orientation. Tipping the crystal by $\pm 10^\circ$ reduced the magnetization at 10 K and 2.0 T by about 5% and tipping by 30° reduced the magnetization by about 25%. When the field was in the a-b plane, the magnetization was rather noisy and highly irreversible so no extensive data are reported here. We assume that the noise arose from bundles of flux jumping from place to place in the crystal.

IV. CONCLUSIONS

$\text{La}_{1.90}\text{Sr}_{0.10}\text{CuO}_4$ is a bulk superconductor that expels flux over the entire H - T plane in a manner similar to the optimally doped cuprate superconductors and the classical type-II superconductors. Normal-state magnetization data in the temperature range from 55 to 200 K obeys 2D Heisenberg antiferromagnetic behavior rather well. This gives a

relatively small background to subtract in the study of the superconducting magnetization. The background also contains a small saturating ferromagnetic term parallel to the c axis that is the same for all temperatures. It saturates at about 0.2 T. There is a large portion of the H - T plane where the magnetization is thermodynamically reversible giving a large region where the free-energy change with magnetic field can be measured. Superconducting magnetization curves are Abrikosov-like for temperatures below 18 K and they show fluctuation behavior above 22 K. The cross-over on the M vs T plot shows $4\pi M^* = -1.13$ G and $T^* = 22.0$ K to give $s = 1.6$ nm compared with the CuO_2 plane spacing of 0.66 nm. The fit of the M vs T data to the model of fluctuating pancake vortices is rather good and gives a crossing point for all fields above 0.5 T. The fit of the reversible magnetization curves to the Hao-Clem model gives a κ_c value of about 175 and a zero temperature thermodynamic critical field of $H_c(0) = 140$ mT. For a T_{co} of 26.8 K, a classical superconductor like tin would have an $H_c(0)$ closer to 300 mT. Hence this underdoped high- T_c material with about 2/3 the optimal carrier density excludes about half the flux expected for a classical superconductor. For classical superconductors, BCS (Ref. 26) predicts the ratio of $H_c(0)/T_{co}$ to be governed by the density of states $N(0)$, by $H_c(0)/T_{co} = 1.75[4\pi N(0)]^{1/2}k_B$. It is not known whether BCS applies here but if it does, one might expect $H_c(0)/T_{co}$

to be reduced as carriers are reduced below optimal doping. For most classical superconductors, the ratio of $H_c(0)/T_{co}$ is about 10 mT/K. For this underdoped high- T_c material the ratio is about 5.4 mT/K which may reflect a relatively small value of $N(0)$ compared to that found for classical superconductors.

The attempt to study fluctuation diamagnetism above T_c was only a partial success. As shown by the magnetization data in Fig. 3, there is a substantial diamagnetic magnetization at 32 K, well above T_c . Indeed the magnetization is diamagnetic all the way to 40 K. Above 40 K, however, the signal is small compared to the background magnetization of the Cu spins. There is sufficient uncertainty in analyzing the background magnetization, that fluctuating diamagnetism in the 40–100 K pseudogap range can not be determined from these data.

ACKNOWLEDGMENTS

We thank C. Song for the x-ray study which showed that the sample was a single crystal and determined the direction of the major axes. Ames Laboratory is operated for the U. S. Department of Energy by Iowa State University under Contract No. W-7405-ENG-82 and supported by the DOE, the Office of Basic Energy Sciences.

-
- ¹T. Timusk and B. Statt, Rep. Prog. Phys. **62**, 61 (1999).
²G. W. Crabtree, W. K. Kwok, L. M. Paulius, A. M. Petrean, R. J. Olsson, G. Karapetrov, V. Tobos, and W. G. Moulton, Physica C **332**, 71 (2000).
³G. Blatter, M. V. Feigel'man, V. B. Geshkenbein, A. I. Larkin, and V. M. Vinokur, Rev. Mod. Phys. **66**, 1125 (1994).
⁴P. H. Kes, C. J. van der Beek, M. P. Maley, M. E. McHenry, D. A. Huse, M. J. Menken, and A. A. Minovsky, Phys. Rev. Lett. **67**, 2383 (1991).
⁵A. A. Abrikosov, Zh. Éksp. Teor. Fiz. **32**, 1442 (1957) [Sov. Phys. JETP **5**, 1174 (1957)].
⁶L. N. Bulaevskii, M. Ledvij, and V. G. Kogan, Phys. Rev. Lett. **68**, 3773 (1992).
⁷Q. Li, M. Suenaga, L. N. Bulaevskii, T. Hikata, and K. Sato, Phys. Rev. B **48**, 13 865 (1993).
⁸U. Welp, W. K. Kwok, R. A. Klemm, V. M. Vinokur, J. Downey, and G. W. Crabtree, Physica C **185-189**, 1785 (1991).
⁹Z. Tesanovic, L. Xing, L. Bulaevskii, Qiang Li, and M. Suenaga, Phys. Rev. Lett. **69**, 3563 (1992); Z. Tesanovic and A. V. Andreev, Phys. Rev. B **49**, 4064 (1994).
¹⁰B. Janossy, D. Prost, S. Pekker, and L. Fruchter, Physica C **181**, 51 (1991).
¹¹B. Janossy, H. Kojima, I. Tanaka, and L. Fruchter, Physica C **176**, 517 (1991); M. Willemin, C. Rossel, J. Hofer, H. Keller, and A. Revcolevschi, Phys. Rev. B **59**, R717 (1999).
¹²J. E. Ostenson, S. Bud'ko, M. Breitwisch, and D. K. Finnemore, Phys. Rev. B **56**, 2820 (1997).
¹³J. E. Ostenson and D. K. Finnemore, Chin. J. Phys. (Taipei) **36**, 297 (1998).
¹⁴C. J. van der Beek, M. Konczykowski, T. W. Li, P. H. Kes, and W. Benoit, Phys. Rev. B **54**, R792 (1996).
¹⁵D. C. Johnston, Phys. Rev. Lett. **62**, 957 (1989).
¹⁶L. J. de Jongh, *Magnetism and Magnetic Materials*, edited by C. D. Graham and J. Rhyne, AIP Conf. Proc. No. 10 (AIP, New York, 1973), p. 561.
¹⁷E. Dagotto, Rep. Prog. Phys. **62**, 1525 (1999); S. Bacci, E. Gagliano, and E. Dagotto, Phys. Rev. B **44**, 285 (1991).
¹⁸A. Revcolevschi and J. Jegoudez, Prog. Mater. Sci. **42**, 321 (1997); S. Petit, A. H. Moudden, B. Hennion, A. Vietkin, and A. Revcolevschi, Eur. Phys. J. B **3**, 163 (1998).
¹⁹M.-H. Julien, F. Borsa, P. Caretta, M. Horvatic, C. Berthier, and C. T. Lin, Phys. Rev. Lett. **83**, 604 (1999).
²⁰T. Nakano, M. Oda, C. Manabe, N. Momono, Y. Miura, and M. Ido, Phys. Rev. B **49**, 16 000 (1994).
²¹V. G. Kogan, M. Ledvij, A. Yu. Simonov, J. H. Cho, and D. C. Johnston, Phys. Rev. Lett. **70**, 1870 (1993).
²²H. Iwasaki, F. Matsuoka, and K. Tanigawa, Phys. Rev. B **59**, 14 624 (1999).
²³J. Mosqueira, M. V. Ramallo, A. Revcolevschi, C. Torron, and F. Vidal, Phys. Rev. B **59**, 4394 (1999).
²⁴Z. Hao and J. R. Clem, Phys. Rev. Lett. **67**, 2371 (1991).
²⁵Qiang Li, M. Suenaga, T. Kimura, and K. Kishio, Phys. Rev. B **47**, 11 384 (1993).
²⁶J. Bardeen, L. N. Cooper, and J. R. Schrieffer, Phys. Rev. **108**, 1175 (1957).